

Kinematic and Dynamic Modeling Based on Trajectory Tracking Control of Mobile Robot with Mecanum Wheels

Hassan M. Alwan^{1*}, Volkov A. Nikolaevic², Sameh F. Hasan¹, Kochneva O. Vladmerovna²

¹*Mechanical Engineering Department, University of Technology, Alsinaa street, 10066, Baghdad, Iraq*

²*High School of Automation and Robotics, Peter the Great St. Petersburg Polytechnic University, 29, Polytekhnicheskaya street, St. Petersburg, 195251, Russia*

Abstract. The trajectory tracking is important to make the WMR move autonomously from the starting point to the destination along a predefined time. Implementing of trajectory tracking control is a fundamental part to accomplish its application tasks. In this article a new method by using a hybrid controller has been presented to solve the problem of the trajectory tracking of four mecanum wheeled mobile robot. Proposed controller is depending on modeling of robot kinematic and dynamic equations. The novelty in this work is that, an optimal control system self-tuning parameters based on an optimization algorithm for these models of the mobile robot is utilized. The optimal control type that is used in this work is the Linear Quadratic Regulator (LQR) controller. LQR is used to control the actuator torque that is required in each wheel to achieve the robot task. The parameters of the LQR controller are tuned by using Ant Colony Optimization (ACO). For results simulation, MATLAB/ Simulink is used for circular and infinity shape trajectories. Results show that when the robot follows a circular trajectory, the values of position trajectory error values are reduced to small value ($e_x=3.218 \times 10^{-5} \text{m}$) and ($e_y= 2.224 \times 10^{-5} \text{m}$) in x_0 and y_0 directions, respectively and remained almost at these values until the end of the simulation time. The maximum orientation error is ($e_\theta= 0.103 \text{rad}$), and convergent to zero after two seconds of the mobile robot movement. Also when the robot follows an infinity shape trajectory, the position trajectory error values are (e_y) and (e_θ) are reduced to small value - $4.078 \times 10^{-4} \text{m}$ and $3.174 \times 10^{-4} \text{rad}$ respectively, while, (e_x) is reduced to $5.263 \times 10^{-4} \text{ m}$ after about 15 seconds.

Keywords: Ant colony optimization; Linear quadratic regulator controller; Robot kinematics: Trajectory tracking; Wheeled mobile robot

1. Introduction

The researches about the control of trajectory tracking of the mobile robot (WMR) are increased dramatically. In their review paper (Abed, Lutfy, and Al-Doori, 2021) presents various trajectory planning strategies for mobile robots using different optimization methods proposed in last year. In their study (Song, Tang, and Li, 2024) addressed the issue of guiding a mobile robot through a dynamic environment by combining the enhanced ant colony optimization ACO with the dynamic window approach DWA algorithm. (Amouri, Cherfia, and Merabti, 2021) proposed a new method to develop kinematic and dynamic

*Corresponding author's email: hassan.m.alwan@uotechnology.edu.iq, Tel.: +9647902597660
doi: [10.14716/ijtech.v15i5.6908](https://doi.org/10.14716/ijtech.v15i5.6908)

models to improve the trajectory tracking accuracy. A new dynamic window algorithm DWA is proposed by [Wang, Ma, and Zhu \(2022\)](#) to set the initial direction angle and then improve its evaluation function during implementation of the trajectory tracking to increase the efficiency and flexibility of the algorithm. A non-singular terminal sliding mode control (NTSMC) was used by [Sun *et al.* \(2020\)](#) for the mobile robot trajectory tracking. Mathematical models of the mobile robot firstly, have been obtained with taking into account the uncertainty effect. An optimal robust control strategy is designed by [\(Chai *et al.*, 2024\)](#) based on the modified backstepping method to achieve stable, accurate and real-time trajectory tracking for the wheeled mobile robot in the presence of unavoidable disturbances. PID and LQR controllers have been proposed by [Amudhan *et al.* \(2019\)](#) to use in path controlling of a four wheeled omnidirectional robot. Circular and rectangular shapes trajectories have been followed in the performance examination of proposed controllers. [Yuan *et al.*, \(2019\)](#) have been applied theoretically and experimentally the extended state observer (ESO) relying on the sliding mode control (SMC) for the trajectory tracking of FMWMR. ESO-SMC based on both kinematic and dynamic models of the WMR was applied with taking into account the effect of the uncertainty and the disturbance. [Morales *et al.* \(2018\)](#) presented the performance analysis of FMWMR experimentally by using linear quadratic regulator (LQR) controller. Control of trajectory tracking of the omnidirectional WMR was solved by using the model predictive control (MPC) based on only the mobile robot kinematic model [\(Wang *et al.*, 2018\)](#). A modified active disturbance rejection control (ADRC) built by [\(Azar *et al.*, 2023\)](#) which includes a nonlinear state error feedback controller and nonlinear tracking differentiator (TD) for the estimation error correction during the trajectory tracking. In work done by [Malayjerdi, Kalani, and Malayjerdi, \(2018\)](#), hybrid controller consisting of self – tuning fuzzy PID controller based on the kinematic model of FMWMR was utilized. In their work, [\(Keek, Loh, and Chong, 2018\)](#) fractional order proportional-integral (FOPI) controller utilized experimentally for the trajectory tracking of the FMWMR was implemented. [\(Khadanga *et al.* 2018\)](#) and [Gao *et al.* \(2017\)](#) studied the wheeled mobile robot trajectory tracking controller design. For the problem of mobile robot's path planning under the known environment, a path planning method of mixed artificial potential field (APF) and ant colony optimization (ACO) based on grid map is proposed by [\(Chen and Liu, 2019\)](#) to explore a new and better path to receive stronger stability and environmental adaptability. The kinematics and dynamics models and proposed Backstepping controller algorithm have been derived for the trajectory tracking of the robot. Both mathematical models for WMR were derived based on the wheels velocities and robot mass centre point velocities. [Hussein \(2023\)](#) presented a new hybrid controller based on both kinematic and dynamic models of a non-holonomic wheeled mobile robot. The gains parameters of the hybrid controller were tuned by applying a modified version of a grey wolf optimization. [Cui *et al.* \(2012\)](#) proposed and simulated results to show the effectiveness of the backstepping-based controller with proven global stability by selecting a Lyapunov function and introducing a virtual control input for the built dynamical model. In their paper [\(El-Shorbagy and Hassanien, 2018\)](#) a comprehensive review of PSO as a well-known population-based optimization technique used in the field of WMR. They start by a brief introduction to the behaviour of the PSO, and then introduced the other representation, convergence properties and the applications of PSO. The aim of their study [\(Heryanto and Kusumoputro, 2021\)](#) was to propose an inner loop control algorithm for UAV using a neural network-based DIC system. The experimental results showed that the neural network-based DIC could follow the manoeuvres of the testing trajectory dataset with excellent performance, as indicated by an overall mean squared error (MSE). [\(Mehenge *et al.*, 2023\)](#) work introduces a three-wheel holonomic omnidirectional robot designed for mobile applications. This platform with three

omnidirectional wheels and DC motors, controlled by EMS 30A H-Bridge and Arduino Mega 2560, it aligns kinematic calculations with mathematical models, promising efficiency for diverse mobile manipulation robot applications. The main contribution of (Mohammed, Al-Khafaji, and Abbas, 2023) paper is to develop an innovative algorithm to accurately detect and identify the shape and color of objects and find their location. The proposed algorithm utilizes the HSV color model to distinguish between different object colors and shapes. After that, a series of filters are applied to reduce the noise of these images to make the process of discovering the shape and coordinates of the objects successful. (Wang *et al.* 2021) review a collision avoidance researches under unknown environments for WMR including various types of controllers. In their approach (Pramujati *et al.*, 2023) introduces a model-based control scheme consists of two systems for controlling the position of a suspended cable-driven parallel robot. Three trajectories are generated to test the compliance of the controller with its position. The error compensation scheme is introduced to increase the positional accuracy of the previous controller, especially on the z-axis. Williams and Wu (2010) have established a novel method of obstacle-avoidance motion planning for mobile robots in dynamic environments, wherein the obstacles are moving with general velocities and accelerations, and their motion profiles are not preknown. A hybrid system is presented in which a global deliberate approach is applied to determine the motion in the desired path line (DPL). Rusdinar *et al.* (2021) developed a mobile robot with a UVC light system installed at the top and bottom to emit UVC light. This robot can be operated automatically as it has a magnetic line sensor and employs a fuzzy inference system algorithm for its movement. The experiment showed that UVC light has good sterilization and disinfection performance.

Finally, it can be concluded that despite many methods are applied in the literature for designing the trajectory tracking control strategy of the WMR for example: Fuzzy logic controller (Rahman, Hassan, and Ihsan, 2022), Adaptive Neuro-Fuzzy Inference System ;(ANFIS) (Tilahun *et al.* 2023), Proportion integral differential (PID)(Saleh, Hussain, and Klim, 2018), linear quadratic regulator (LQR) (Uddin, 2018), model predictive control (MPC), etc, but they have drawbacks such as large computational burden and long convergence time when dealing with under actuated system. In addition, sliding model control (SMC) is another effective method, but the chattering phenomenon limits its application.

In this work, hybrid controllers based on kinematics and dynamics are designed to solve the trajectory tracking problem of a four mecanum wheeled mobile robot. The type of the optimal control is the Linear Quadratic Regulator controller (LQR). LQR is applied to design the controlled torques required by actuators and parameters of LQR controller are tuned by using Ant Colony Optimization (ACO).

2. Kinematic and dynamic mathematical models of mobile robot

To derive mobile robot kinematic and dynamic mathematical models, velocities of its centre in local coordinates system $V_r = (V_{rx} \ V_{ry} \ \dot{\theta})^T$ will be adopted with respect to angular velocities and torques of the wheels. The rotation of each wheel is achieved by a separate motor, while the wheels passive rollers have been driven by the frictional force with the ground. The top view configuration of proposed mobile robot (FMWMR) is shown in Figure 1a. It is noted that, the origin point of mobile robot local coordinate system does not coincide with the whole mobile robot mechanism mass center (point D).

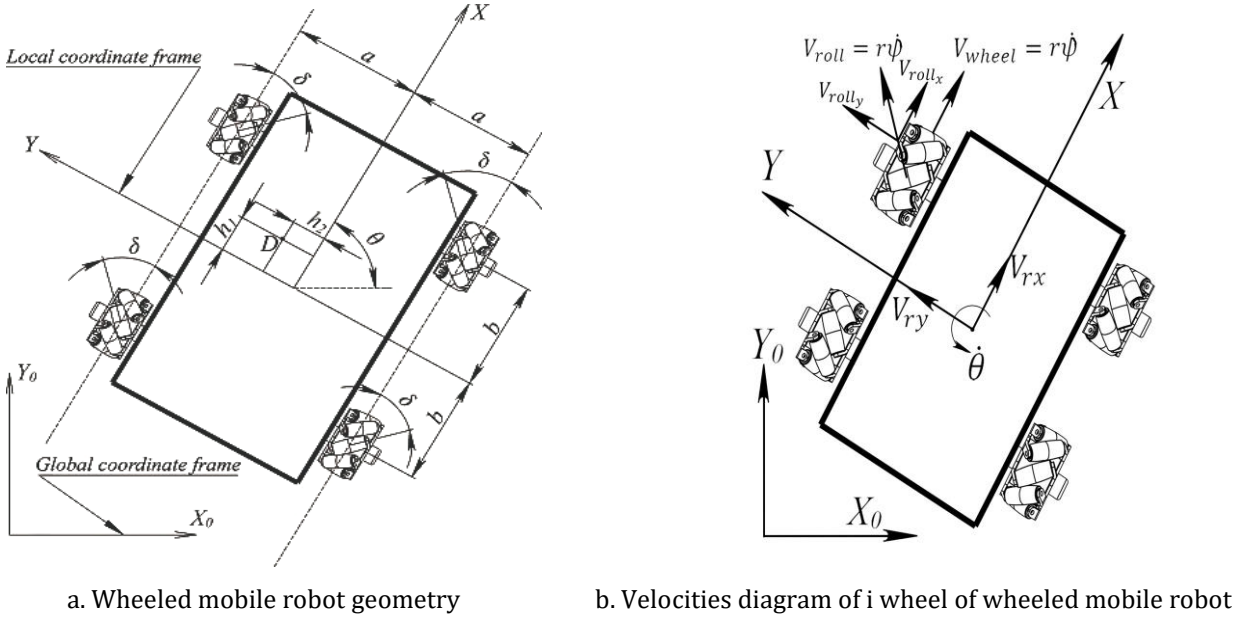


Figure 1 Kinematic model of proposed wheeled mobile robot

Referring to i wheel of the mobile robot Figure 1b, wheel radius is r_{wi} , its angular velocity is $\dot{\phi}_i$ and its linear velocity resulted from the wheel rotation is $v_{wi} = r_{wi}\dot{\phi}_i$. Also the linear velocity of each passive roller is referred by $V_{i\text{roller}}$ which is equal to v_{wi} and perpendicular on the roller axis [Hasan and Alwan, 2022].

In this scenario, the mobile robot is viewed as a complete mechanism with the angular velocities of its wheels serving as inputs and the robot's linear and angular velocities as outputs. In this context the Jacobian matrix of inverse kinematics can be expressed as (Equation 1):

$$J = \frac{1}{r_{wi}} \begin{bmatrix} 1 & -1 & -(a+b) \\ 1 & 1 & (a+b) \\ 1 & 1 & -(a+b) \\ 1 & -1 & (a+b) \end{bmatrix} \quad (1)$$

FMWMR inverse kinematic equation in robot local coordinate system is expressed as below (Equation 2):

$$\dot{\phi} = JV_r \quad (2)$$

Where: $\dot{\phi} = (\dot{\phi}_1 \ \dot{\phi}_2 \ \dot{\phi}_3 \ \dot{\phi}_4)^T$ is the Matrix of angular velocities of all robot mecanum wheels. Taking in account that $V_{rg} = (\dot{x}_o \ \dot{y}_o \ \dot{\theta})^T$ is the robot velocities in global coordinate system, equation of inverse kinematic can be written as follow in global coordinate system (Equation 3):

$$\dot{\phi} = J R_L^G V_{rg} \quad (3)$$

Where R_L^G matrix of robot local coordinates system rotation with reference to global coordinates system, and will be presented (Equation 4):

$$R_L^G = \begin{bmatrix} \cos\theta & \sin\theta & 0 \\ -\sin\theta & \cos\theta & 0 \\ 0 & 0 & 1 \end{bmatrix} \quad (4)$$

The forward kinematic jacobian matrix (J^+) is pseudo-inverse of (J) [Zeidis et al. 2019], its formula was written as: $J^+ = (J^T J)^{-1} J^T$. The forward kinematics equation in robot local coordinates system is written (Equation 5):

$$V_r = J^+ \dot{\phi} \quad (5)$$

The forward kinematics equation for the FMWMR in global coordinate system can be written as follow (Equation 6):

$$V_{rg} = R_L^G J^+ \dot{\phi} \quad (6)$$

In the Lagrange formulation, the dynamic model of the robot includes the motion of the system resulting from the inertia of the entire robot mechanism and external forces. As illustrated in Figure (1a), point C represents the centre of the robot's local coordinate frame, and (D) is the mass centre of the entire robot mechanism.

Velocity of local coordinate system origin point of the FMWMR (point C) in robot local coordinate system is evaluated according to the theory in as (Equation 7):

$$v_C = \begin{bmatrix} \cos\theta & \sin\theta \\ -\sin\theta & \cos\theta \end{bmatrix} \begin{bmatrix} \dot{x}_o \\ \dot{y}_o \end{bmatrix} \quad (7)$$

where, \dot{x}_o and \dot{y}_o are mass centre point velocities point (C) in global coordinate system, (θ) is rotation angle of robot local coordinate frame relative to global coordinate frame. Also, the velocity component of point (D) in the local system has been expressed as (Equation 8):

$$v_D = v_C + \dot{\theta}_K \times \vec{r}_D \quad (8)$$

Since the robot cannot change its vertical position (z-axis), so its potential energy is equal to zero. The kinetic energy of the whole robot mechanism includes the kinetic energy of the four mecanum wheels and robot platform. In this case L is only kinetic energy of the robot and has been written as (Equation 9):

$$L = T = \frac{1}{2} [m_r v_D^T v_D + I_r \dot{\theta}^2 + \sum_{i=1}^4 m_{wi} (r \dot{\phi})^2] + \sum_{i=1}^4 I_{wi} (\dot{\phi})^2 \quad (9)$$

Where: m_r : mass of robot platform , m_{wi} : mass of i wheel, I_r : Robot mass moment of inertia about its centre of mass point, I_{wi} : moment of inertia of i wheel. The Lagrange equation derived from the total energy of the whole robot will present the dynamic model and can be written as (Equation 10):

$$\frac{d}{dt} \left(\frac{\partial L}{\partial \dot{\phi}_i} \right) - \left(\frac{\partial L}{\partial \phi_i} \right) = F_i, \quad i=1,2,3 \quad (10)$$

The general form of the robot dynamic equation can be written (Equation 11):

$$M(q)\ddot{q} + C(q, \dot{q})\dot{q} + B^T S f = \frac{1}{r} B^T \tau \quad (11)$$

Where: $\dot{q} = (\dot{x}_o \quad \dot{y}_o \quad \dot{\theta})^T$, $\ddot{q} = (\ddot{x}_o \quad \ddot{y}_o \quad \ddot{\theta})^T$

Mass and inertia matrix [M] can be written (Equations 12, 13, 14, 15 and 16):

$$M = \begin{bmatrix} M_{11} & M_{12} & M_{13} \\ M_{21} & M_{22} & M_{23} \\ M_{31} & M_{32} & M_{33} \end{bmatrix}, \quad (12)$$

$$M_{11} = M_{12} = 4 \left(m_{wi} + \frac{I_{wi}}{r_{wi}^2} \right) + m_r \quad (13)$$

$$M_{13} = M_{31} = m_r (h_1 \sin\theta + h_2 \cos\theta) \quad (14)$$

$$M_{23} = M_{32} = m_r (h_1 \cos\theta + h_2 \sin\theta) \quad (15)$$

$$M_{33} = m_r (h_1^2 + h_2^2) + I_r + 4 \left(m_{wi} + \frac{I_{wi}}{r_{wi}^2} \right) (a + b)^2 \quad (16)$$

Matrix of carioles and centripetal effect [C], [f] is vector of the friction force and [B] is input transformation matrix. The elements of each matrix are represented as (Hasana and Alwan, 2021) (Equations 17, 18 and 19):

$$C = \begin{bmatrix} 0 & 0 & m_r\dot{\theta}(h_1\cos\theta + h_2\sin\theta) \\ 0 & 0 & m_r\dot{\theta}(h_1\sin\theta + h_2\cos\theta) \\ 0 & 0 & 0 \end{bmatrix} \quad (17)$$

$$B = \begin{bmatrix} (\cos\theta + \sin\theta) & (\sin\theta - \cos\theta) & -(a+b) \\ (\cos\theta - \sin\theta) & (\sin\theta + \cos\theta) & (a+b) \\ (\cos\theta - \sin\theta) & (\sin\theta + \cos\theta) & -(a+b) \\ (\cos\theta + \sin\theta) & (\sin\theta - \cos\theta) & (a+b) \end{bmatrix} \quad (18)$$

$$S = \begin{bmatrix} \operatorname{sgn}(\dot{\phi}_1) & 0 & 0 & 0 \\ 0 & \operatorname{sgn}(\dot{\phi}_2) & 0 & 0 \\ 0 & 0 & \operatorname{sgn}(\dot{\phi}_3) & 0 \\ 0 & 0 & 0 & \operatorname{sgn}(\dot{\phi}_4) \end{bmatrix} \quad (19)$$

3. Controller design for trajectory tracking

In this section, a control system with self-tuning parameters based on an optimization algorithm is utilized for both robot models. The type of the optimal control that is used in this work is the Linear Quadratic Regulator controller (LQR). It is used to design the controlled torques generated by the wheels motors. The parameters of the LQR controller are tuned by using Ant Colony Optimization (ACO) and this matter is presented in the next subsections.

3.1. Linear quadratic regulator controller (LQR)

This controller is considered to be a type of an optimal control system. It is used in a lot of applications such as robot actuators control and in airplane flight control. The main objective of LQR controller usage is getting optimal control signal of the generated torques. The state space representation of the robot system (Equations 20 and 21):

$$X = AX + BU \quad (20)$$

$$Y = CX \quad (21)$$

where (X) represents the state-space vector and (U) is the torque control signal. The feedback control law when taking (K) the gain vector is (Equation 22):

$$U = -KX \quad (22)$$

In this work, the equation of the cost function is proposed Equation 23):

$$G = \int_0^{\infty} (X^T Q X + U^T R U) d \quad (23)$$

Where: (R) is the symmetric positive definite matrix and (Q) the symmetric positive semi-definite matrix. Elements of (R) and (Q) matrices (Equations 24 and 25):

$$Q = \begin{bmatrix} Q_1 & 0 & 0 & 0 \\ 0 & Q_2 & 0 & 0 \\ 0 & 0 & Q_3 & 0 \\ 0 & 0 & 0 & Q_4 \end{bmatrix} \quad (24)$$

$$R = \begin{bmatrix} R_1 & 0 & 0 & 0 \\ 0 & R_2 & 0 & 0 \\ 0 & 0 & R_3 & 0 \\ 0 & 0 & 0 & R_4 \end{bmatrix} \quad (25)$$

The equation of the optimal feedback is evaluated as (Equation 26):

$$K = R^{-1}B^TP \quad (26)$$

where (P) is defined as the Riccati equation which is calculated (Equation 27):

$$A^TP + PA + Q - PBR^{-1}B^TP = 0 \quad (27)$$

The equation of the control law is introduced (Equation 28):

$$U = -KX + VY_d \quad (28)$$

where $V = -(C^T(A - BK)^{-1}B)^{-1}$ to be sure that the steady state error becomes zero.

LQR controller used in this work is adopted to make an optimal control signal for the motors torques.

3.2. Ant colony optimization (ACO)

[Pei, Wang, and Zhang \(2012\)](#) states that, ACO type of optimization is an intelligent heuristic algorithm which was developed in 1992 by Marco Dorigo which simulates from the ant foraging behaviour. The communication between ants is relying on the pheromones and the pheromones are proportional inversely with length of the path. During the searching of the ants for the food in an unknown environment, ants have been moved threw a path containing a high pheromone concentration. Concentration of pheromone is directly proportional with the numbers of the ants that walking on this path. Ants behaviours display the principle in which adopted to select an optimal path. To enhance path planning efficiency, heuristic function (η) and tabu list (tabu_k) are adopted into an artificial ant colony model. Within a time (t), ant k moves from a current node i to an unvisited node j regarding the distance information received from the target point and pheromone intensity during this path. In the case of more than one unvisited node, the transition probability (P_{ij}^k) between the nodes will be evaluated by the ant K in accordance with the formula that shown (Equation 29) :

$$P_{ij}^k = \left\{ \frac{[\cap_{ij}(t)]^\alpha [\varepsilon_{ij}(t)]^\beta}{\sum_{s \in U} [\cap_{ij}(t)]^\alpha [\varepsilon_{ij}(t)]^\beta} \right\} \quad (29)$$

where U represents the next node of ant k , β is an expectation heuristic factor, α is a pheromone heuristic factor, $[\cap_{ij}(t)]$ is a pheromone concentration on the path ij at a period of time (t), $\varepsilon_{ij}(t)$ is an expected heuristic functio a (Equation 30):

$$\varepsilon_{ij} = \frac{1}{d_{ij}} \quad (30)$$

where d_{ij} is a Euclidean distance between any two adjacent nodes. After finishing the path search by all ants, pheromone was evaporated. The formula that describes the increasing of the pheromone on the path (Equations 31 and 32):

$$\cap_{ij}(t+1) = (1 - \rho) \cap_{ij}(t) + \Delta \cap_{ij} \quad (31)$$

$$\Delta \cap_{ij} = \sum_{K=1}^m \Delta \cap_{ij}^K(t) \quad (32)$$

where (ρ) represents the rate of the pheromone evaporation, and (t) is the time of the iterations. Value of $\Delta \cap_{ij}^K(t)$ depends on the pheromone addition which has been done by an ant (K) after its movement on (ij) path during iteration time (t). Mathematical model of $\Delta \cap_{ij}^K(t)$ can be defined as (Equation 33):

$$\Delta \cap_{ij}^K = \begin{cases} \frac{N}{L_K}, & \text{tour}(i,j) \in \text{tour}_K \\ 0, & \text{otherwise} \end{cases} \quad (33)$$

Where (N) represents the intensity of the pheromone that added by the ant (K) and (L_K) represents the length of the path that was tracking by the ant (K) during one iteration. There is no fixed rule to choose the ant's number as well as the Max. number of iteration. The selection number is considered to be acceptable because the higher number of iterations and ants required more program execution time. Also, it is needed a computer with high specifications. The basic parameters for the ACO have been chosen as follow:

Ants Number: 30

Max. Iteration Number: 100

Objective Function: $\sqrt{\frac{1}{N} \sum_{i=1}^m (e_x^2 + e_y^2 + e_\theta^2)}$

The tracking error between the desired trajectory and actual trajectory at any point can be presented as (Equation 34):

$$e = (e_x \ e_y \ e_\theta)^T = \begin{pmatrix} x_d - x_{ac} \\ y_d - y_{ac} \\ \theta_d - \theta_{ac} \end{pmatrix} \quad (34)$$

In this work, ACO is adopted in selection of optimal values of (Q) and (R) matrices elements. In simulation work, a closed loop controller (Figure 2) has been implemented. This loop is a trajectory tracking controller based on minimizing the pose error to zero. We used LQR controller where the gains were obtained by using Anti Colony Optimization ACO to control the motors torques.

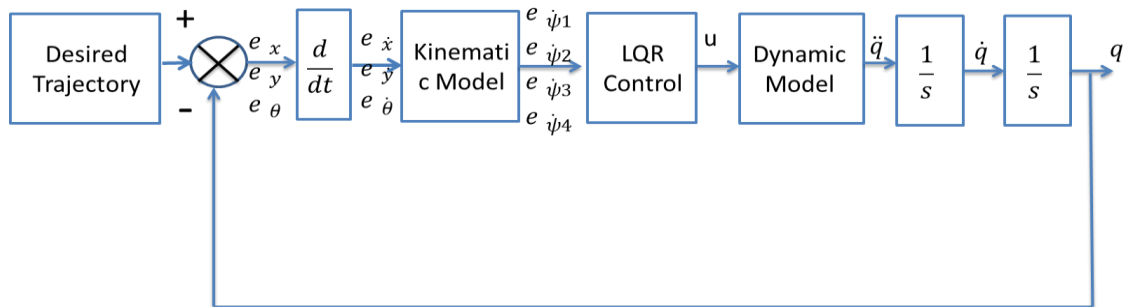


Figure 2 Controller architecture

4. Results and discussion

The proposed controller has been examined in two options of WMR movement. In first option WMR follows a circular shape trajectory and in second option it follows an infinity shape trajectory. The results have been simulated by using MATLAB 2019 software. The parameters of robot are taken as follow:

$M=8 \text{ kg}$, $I_b=0.2 \text{ kg m}^2$, $I_w=0.1 \text{ kg m}^2$, $r_{wi}=0.05 \text{ m}$, $h_1=0.35 \text{ m}$, $h_2=0.25 \text{ m}$, $\mu=0.01$. The ranges of the elements in the (Q) and (R) matrices fall between 0 and 30. Various values of these elements were tested to minimize the overall cost function while ensuring reliable controller performance. The selected values of these elements were evaluated using ACO and are presented as (Equations 35 and 36):

$$Q = \begin{bmatrix} 12.59 & 0 & 0 & 0 \\ 0 & 27.35 & 0 & 0 \\ 0 & 0 & 18.22 & 0 \\ 0 & 0 & 0 & 14.87 \end{bmatrix} \quad (35)$$

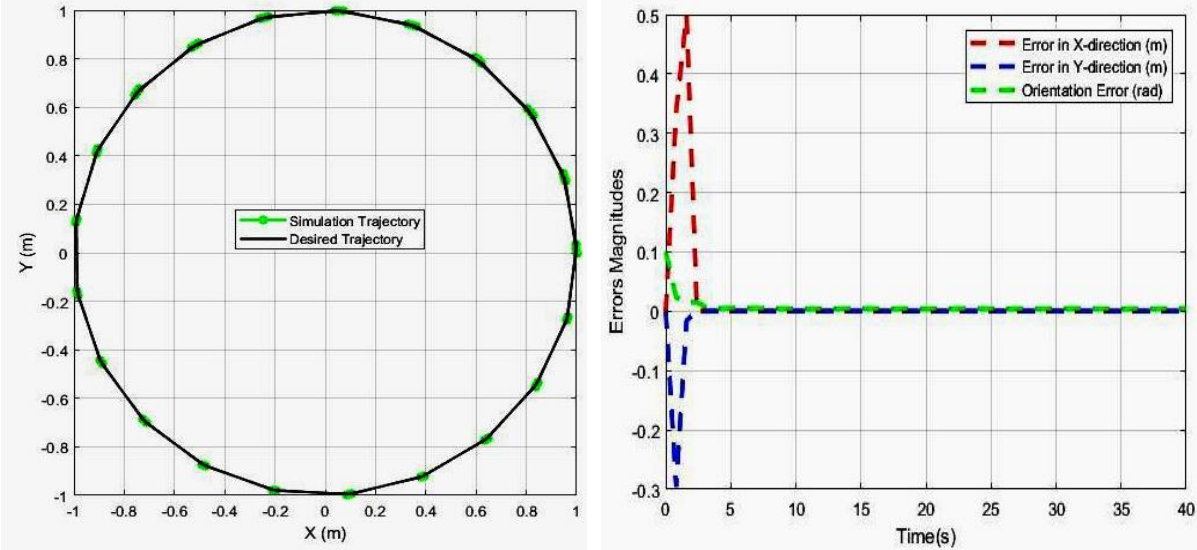
$$R = \begin{bmatrix} 4.36 & 0 & 0 & 0 \\ 0 & 5.88 & 0 & 0 \\ 0 & 0 & 7.21 & 0 \\ 0 & 0 & 0 & 7.28 \end{bmatrix} \quad (36)$$

In the first case, the equations of the circular shape trajectory followed by the WMR are described as (Equations 37 and 38):

$$x_d(t) = \cos(0.4t) \quad (37)$$

$$y_d(t) = \sin(0.4t) \quad (38)$$

The robot movement has been begun from initial point with coordinates $q = (1 \ 0 \ \pi/2)^T$. The performance of the generated trajectory is displayed in Figure 3a. The trajectory tracking errors at any time can be presented as in Figure 3b.



a. Set-point tracking along the circular shape trajectory followed by WMR

b. Trajectory tracking error in case of circular shape followed by WMR

Figure 3 The first proposed circular Shape Trajectory followed by the WMR

After two seconds of the WMR task starting, the values of position trajectory error values are reduced to small value ($e_x = 3.218 \times 10^{-5}$ m) and ($e_y = 2.224 \times 10^{-5}$ m) in x_0 and y_0 directions, respectively and remained almost at these values until the end of the simulation time. The maximum orientation error is ($e_\theta = 0.103$ rad), and convergent to zero after two seconds of the mobile robot movement. Figure 4a shows the robot linear and angular velocities in global coordinate system during the circular trajectory. As shown in Figure 4a the robot velocities behaviour is smooth during the simulation time. The value of the linear velocities is fluctuated about ± 0.4 m/s and robot rotation velocity is 0.4 rad/s. Generated torques from robot mecanum wheels motors can be evaluated at any time. The torques values have been shown in Figure 4b.

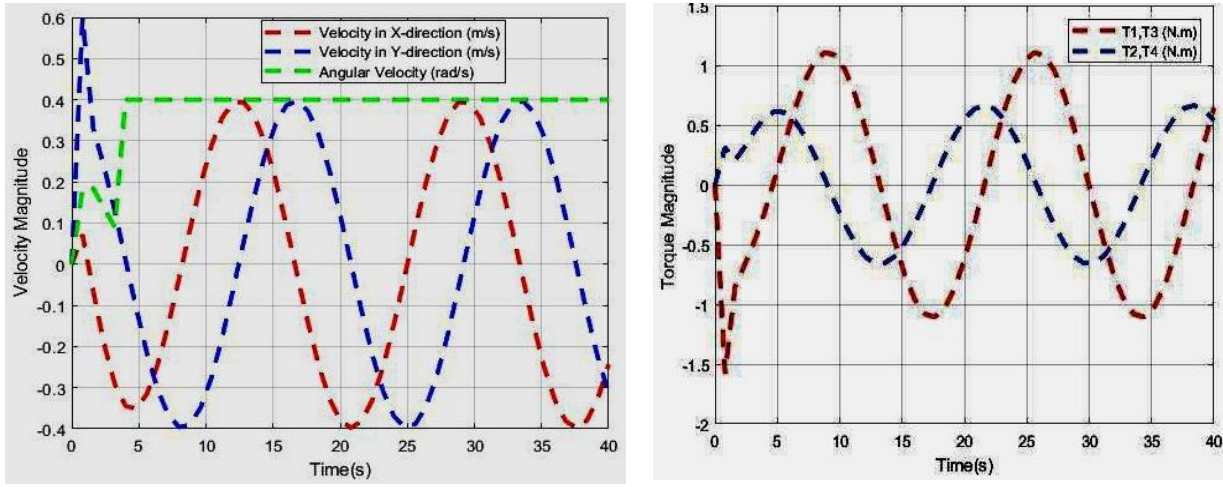
In the second option, the equations of the infinity shape trajectory followed by the WMR are described as (Equations 39 and 40):

$$x_d = 1\sin(0.2t) \quad (39)$$

$$y_d = 1\sin(0.4t) \quad (40)$$

The matching between the desired and theoretical trajectories of the WMR is shown in Figure 5a. The position trajectory error values after three seconds of the task starting, are (e_y) and (e_θ) are reduced to small value -4.078×10^{-4} m and 3.174×10^{-4} rad respectively, while, (e_x) is reduced to 5.263×10^{-4} m after about 15 seconds. The trajectory tracking errors for the infinity shape trajectory followed by WMR at any time can be presented as in Figure

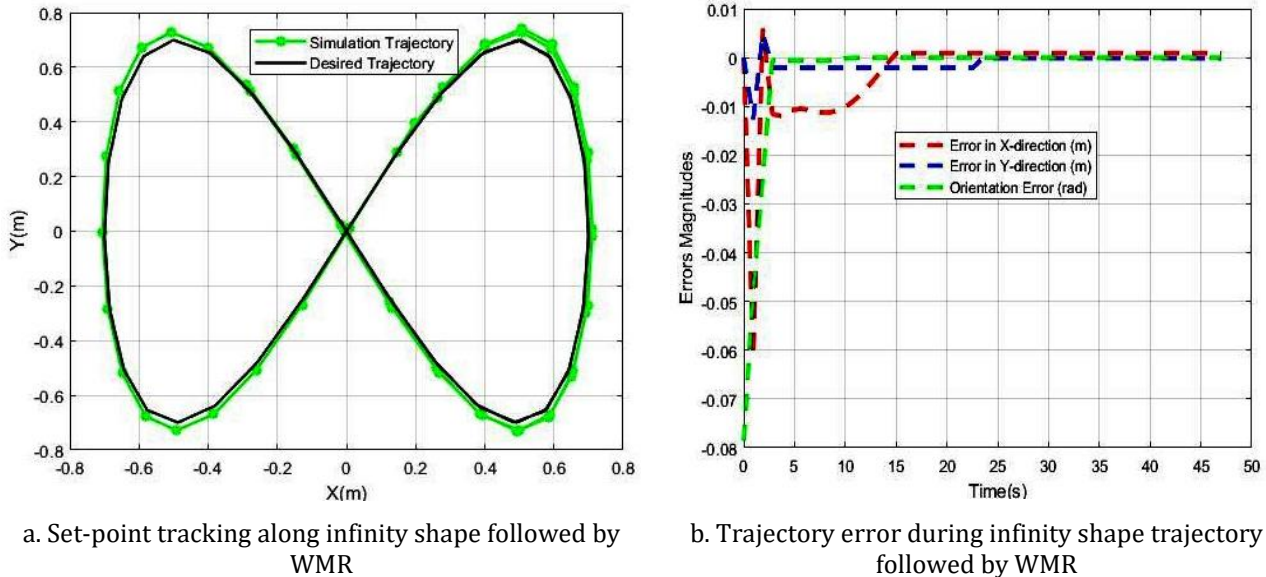
5b. Linear and angular velocities of the center point of mass of the WMR in the global coordinate system shown in Figure 6a. The generated torques from the wheels motors can be evaluated at any time. The values of the torques present in Figure 6b.



a. Generated velocities in WMR wheels when the WMR follows a circular shape trajectory

b. Generated torques in WMR wheels when the WMR follows a circular shape trajectory

Figure 4 Velocities and torques generated in all wheels when the WMR follows a circular shape trajectory

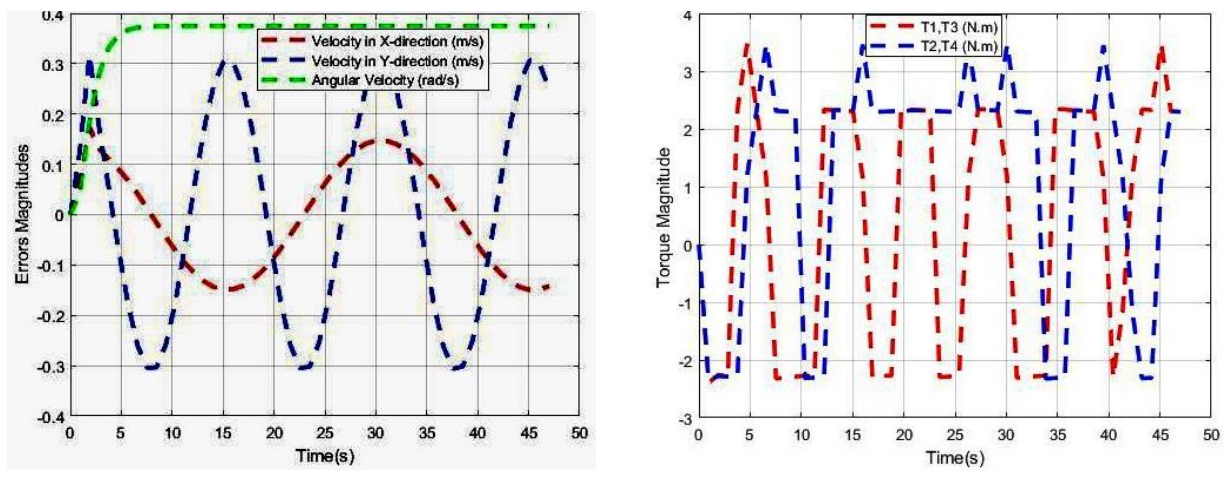


a. Set-point tracking along infinity shape followed by WMR

b. Trajectory error during infinity shape trajectory followed by WMR

Figure 5 The second proposed Infinity Shape Trajectory followed by WMR

It has been seen, in the two cases, simulation results show higher precision of trajectory tracking because the position tracking errors (x, y) are less than $10^{-3}m$ and acceptable comparing with most of published researches.



a. Generated velocities in WMR wheels when the WMR follows an infinity shape trajectory

b. Generated torques in WMR wheels when the WMR follows an infinity shape trajectory

Figure 6 Velocities and torques generated in all wheels when the WMR follows an infinity shape trajectory

5. Conclusions

In this work, an optimal control system is applied based on the kinematics and dynamics of the four mecanum wheeled mobile robot for the trajectory tracking. MATLAB software is used for results simulation of the proposed controller in two cases. In the first case the robot followed a circular shape trajectory and in the second case followed an infinity shape trajectory. The most important points are presented as: LQR controller with a self-tuning parameters based on ACO are applied to control the robot motors torques. In the first case, the values of the trajectory errors in x_0 and y_0 directions are $e_x = 4.645 \times 10^{-4}$ m and $e_y = 7.382 \times 10^{-5}$ m respectively and these values converge to zero after two seconds. In second case, maximum absolute values of the trajectory error (e_x), (e_y) and (e_θ) are 0.05 (m), 0.01 (m), and 0.08 (rad) respectively. After about three seconds, (e_y) and (e_θ) are reduced to small value -4.078×10^{-4} (m) and 3.174×10^{-4} (rad) respectively, while (e_x) is reduced to 5.263×10^{-4} (m) after about 15 sec. The magnitudes of the torques are between (± 1.5) N/m.

Acknowledgments

Authors are pleased to express special appreciations and thanks to "Mechanical Engineering Department at University of Technology, Baghdad, Iraq" and "High School of Automation and Robotics at Peter the Great Saint Petersburg Polytechnic University" for their help and support during the research period.

Nomenclature

WMR	Wheeled Mobile Robot
FMWMR	Four Mecanum Wheeled Mobile Robot
LQR	Linear Quadratic Regulator
ACO	Ant Colony Optimization
DWA	Dynamic Window Approach
NTSMC	Non-Singular Terminal Sliding Mode Control
PID	Proportional Integral Derivative
ESO	Extended State Observer

SMC	Sliding Mode Control
MPC	Model Predictive Control
FOPI	Fractional Order Proportional-Integral

References

Abed, M.S., Lutfy, O.F., Al-Doori, Q.F., 2021. A Review on Path Planning Algorithms for Mobile Robots. *Engineering and Technology Journal*, Volume 39(5), pp. 804–820

Alwan, H.M., 2020. Kinematic Modeling and simulation of Holonomic Wheeled Mobile Robot with Mecanum Wheels. *Journal of Mechanical Engineering Research and Developments*, Volume 43(5), pp. 451–459

Amouri, A., Cherfia, A., Merabti, H., 2022. Nonlinear Model Predictive Control of a Class of Continuum Robots Using Kinematic and Dynamic Models. *FME Transactions*, Volume 50(2), pp. 339–350

Amudhan, A.N., Sakthivel, P., Sudheer, A.P., Kumar, T.S., 2019. Design of Controllers for Omnidirectional Robot Based on the System Identification Technique for Trajectory Tracking. *Journal of Physics: Conference Series*, Volume 1240(1), p. 012146

Azar, A.T., Abed, A.M., Abdul-Majeed, F.A., Hameed, I.A., Jawad, A.J.M., Abdul-Adheem, W.R., Ibraheem, I.K., Kamal, N.A., 2023. Design and Stability Analysis of Sliding Mode Controller for Non-Holonomic Differential Drive Mobile Robots. *Machines*, Volume 11, p. 470

Chai, B., Zhang, K., Tan, M., Wang, J., 2024. An Optimal Robust Trajectory Tracking Control Strategy for the Wheeled Mobile Robot. *International Journal of Control, Automation and Systems*, Volume 22(3), pp. 1050–1065

Chen, G., Liu, J., 2019. Mobile Robot Path Planning Using Ant Colony Algorithm and Improved Potential Field Method. *Computational Intelligence and Neuroscience Journal*, Volume 12, pp. 1–10

Cui, Q.Z., Li, X., 2012. Backstepping Control Design on the Dynamic of Omni-Directional Mobile Robot. *Journal of Applied Mechanics and Materials*, Volume 203, pp. 51–56

El-Shorbagy, M.A., Hassanien, A.E., 2018. Particle Swarm Optimization from Theory to Applications. *International Journal of Rough Sets and Data Analysis*, Volume 5(2), pp. 1–14

Gao, Z., Yang, Y., Du, Y., Zhang, Y., Wang, Z., Xu, W., 2017. Kinematic Modeling and Trajectory Tracking Control of a Wheeled Omni-directional Mobile Logistics Platform. In: Asia-Pacific Engineering and Technology Conference (APETC), pp. 169–175

Hasan, S.F., Alwan, H.M., 2022. Local Path Planning of a Four Mecanum Wheeled Mobile Robot Based on New Modified Ultrasonic Sensors with Experimental Implementation. *International Journal of Mechanical Engineering*, Volume 7(1), pp. 4621–4627

Hasana, S.F., Alwan, H.M., 2021. Modelling and Control of Wheeled mobile Robot with Mecanum Wheels. *Engineering and Technology journal*, Volume 39(A), pp. 779–789

Heryanto, M.A., Kusumoputro, B., 2021. Attitude and Altitude Control of Quadcopter Maneuvers using Neural Network-Based Direct Inverse Control. *International Journal of Technology*, Volume 12(4), pp. 843–853

Hussein, R.M., 2023. Design a New Hybrid Controller Based on an Improvement Version of Grey Wolf Optimization for Trajectory Tracking of Wheeled Mobile Robot. *FME Transactions*, Volume 51(2), pp. 140–148

Keek, J.S., Loh, S.L., Chong, S.H., 2018. Fractional-Order Proportional-Integral (FOPI) Controller for Mecanum-Wheeled Robot (MWR) in Path-Tracking Control. *International Journal of Mechanical Engineering and Technology (IJMET)*, Volume 9(11), pp. 325–337

Khadanga, R.K., Padhy, S., Panda, S., Kumar, A., 2018. Design and Analysis of Tilt Integral Derivative Controller for Frequency Control in an Islanded Microgrid: A Novel Hybrid

Dragonfly and Pattern Search Algorithm Approach. *Arabian Journal for Science and Engineering*, Volume 43 (6), pp. 1–12

Malayjerdi, E., Kalani, H., Malayjerdi, M., 2018. Self-Tuning Fuzzy PID Control of a Four-Mecanum Wheel Omni-directional Mobile Platform. *26th Iranian Conference on Electrical Engineering(ICEE)*, Volume 2018, pp. 816–820

Mehenge, R., Satoskar, N., Shidhore, A., Arshath, N.M., 2023. Kinematic and Optimal design of a Three-wheeled Holonomic Omnidirectional Robot Platform for Mobile Manipulation Tasks. *Global Journal of Engineering and Technology Advances*, Volume 17(1), pp. 45–54

Mohammed, M.M., Al-Khafaji, M.M., Abbas, T.F., 2023. Smart Robot Vision for A Pick and Place Robotic System. *Engineering and Technology Journal*, Volume 41(6), pp. 756–770

Morales, S., Magallanes, J., Delgado, C., Canahuire, R., 2018. LQR Trajectory Tracking Control of an Omnidirectional Wheeled Mobile Robot. In: IEEE 2nd Colombian Conference on Robotics and Automation (CCRA), pp. 1–5

Pei, Y., Wang, W., Zhang, S., 2012. Basic Ant Colony Optimization. In: International Conference on Computer Science and Electronics Engineering, Hangzhou, pp. 665–667

Pramujati, B., Syamlan, A.T., Nurahmi, L., Tamara, M.N., 2023. Study on the Application of Model-based Control Algorithm for a Suspended Cable-Driven Parallel Robot. *International Journal of Technology*. Volume 14(4), pp. 854–866

Rahman, A., Hassan, N., Ihsan, S.I., 2022. Fuzzy Logic Controlled Two Speed Electromagnetic Gearbox for Electric Vehicle. *International Journal of Technology*. Volume 13(2), pp. 297–309

Rusdinar, A., Purnama, I., Fuadi, A.Z., Adiluhung, H., Wicaksono, M., Risnanda, Ningrum, R.A., 2021. Automated Ultraviolet C Light Mobile Robot for Room Sterilization and Disinfection. *International Journal of Technology*, Volume 12(4), pp. 854–864

Saleh, A., Hussain, M., Klim, S., 2018. Optimal Trajectory Tracking Control for A Wheeled Mobile Robot Using Fractional Order PID Controller. *Journal of University of Babylon*, Vvolume 26, pp. 292–306

Song, B., Tang, S., Li, Y., 2024. A New Planning Integrating Improved ACO and DWA Algorithms for Mobile Robots in Dynamic Environments. *Mathematical and Biosciences and Engineering Journal*, Volume 21(2), pp. 2189–2211

Sun, Z., Xie, H., Zheng, J., Man, Z., He, D., 2020. Path-following Control of Mecanum-Wheels Omnidirectional Mobile Robots Using Nonsingular Terminal Sliding Mode. *Mechanical Systems and Signal Processing*, Volume 147, p. 107128

Tilahun, A.A., Desta, T.W., Salau, A.O., Negash, L., 2023. Design of an Adaptive Fuzzy Sliding Mode Control with Neuro-Fuzzy System for Control of a Differential Drive Wheeled Mobile Robot. *Cogent Engineering*, Volume 10(2), p. 2276517

Uddin, N., 2018. Trajectory Tracking Control System Design for Autonomius Two-Wheeled Robot. *Journal Infotel*, Volume 10(3), pp. 90–97

Wang, C., Liu, X., Yang, X., Hu, F., Jiang, A., Yang, C., 2018. Trajectory Tracking of an Omni-Directional Wheeled Mobile Robot Using a Model Predictive Control Strategy. *Applied Science*, Volume 8(2), p. 231

Wang, H., Ma, X., Zhu, L., 2022. Obstacle Avoidance Path Planning of Mobile Robot Based on Improved DWA. *Journal of Physics: Conference Series*, Volume 2383(1), p. 012098

Wang, Y., Li, X., Zhang, J., Li, S., Xu, Z., Zhou, X., 2021. Review of Wheeled Mobile Robot Collision Avoidance under Unknown Environment. *Science Progress Journal*, Volume 104(3), pp. 1–26

Williams, R.L., Wu, J., 2010. Dynamic Obstacle Avoidance for An Omnidirectional Mobile Robot. *Journal of Robotics*, Volume 2010, p. 901365

Yuan, Z., Tian, Y., Yin, Y., Wang, S., Liu, J., Wu, L., 2019. Trajectory Tracking Control of a Four Mecanum Wheeled Mobile Platform: an Extended State Observer-Based Sliding Mode Approach. *IET Control Theory & Applications*, Volume 14(3), pp. 415–426

Yuan, Z., Tian, Y., Yin, Y., Wang, S., Liu, J., Wu, L., 2019. Trajectory Tracking Control of a Four Mecanum Wheeled Mobile Platform: an Extended State Observer-Based Sliding Mode Approach. *IET Control Theory & Applications*, Volume 14(3), pp. 415–426

Zeidis, I., Zimmermann, K., 2019. Dynamic of Four Wheeled Mobile Robot with Mecanum Wheels. *Journal of Applied Mathematics and Mechanics*, Volume 3, pp. 1–22